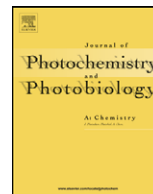




Contents lists available at ScienceDirect

Journal of Photochemistry and Photobiology A: Chemistry

journal homepage: www.elsevier.com/locate/jphotochem

Fourier transform infrared study of mercury interaction with carboxyl groups in humic acids

M.C. Terkhi^a, F. Taleb^a, P. Gossart^b, A. Semmoud^b, A. Addou^{a,*}^a Laboratory of STEVA, Department of Engineering Chemistry, BP 188, University of Mostaganem, Mostaganem, 27000, Algeria^b Laboratory of Infrared and Raman Spectrochemistry (LASIR), University of Sciences and Technology, 59655, Villeneuve d'Ascq, France

ARTICLE INFO

Article history:

Received 8 October 2007
 Received in revised form 17 March 2008
 Accepted 18 March 2008
 Available online 8 April 2008

Keywords:

Humic acid
 Mercury interaction
 Infrared spectroscopy
 ICP-AES
 Contamination

ABSTRACT

An interaction between humic acid, an organic part of soil and mercury was studied by Fourier transform infrared spectroscopy (FTIR) and by ICP-AES analysis under given pH and concentration conditions. First the spectroscopic model was validated on the interaction of simple molecules representing the structural components of humic acid such as benzoic acid, catechol and salicylic acid with mercury. The interaction of carboxylic parts of humic acid with mercury is very interesting and easily characterised by infrared spectroscopy, an ideal mean for molecular study. Under the salt form (commercial humic acid Fluka TM: FHA), humic acid reacts with mercury in a different way from its acid form (FHA purified noted PFHA) and the Leonardite (LHA). Because of the straightforward exchange between Na⁺, Ca²⁺ and Hg²⁺, fixation of the latter is much more important with the salt form (FHA). However, this reaction is reduced under the acid form (PFHA, LHA) because the exchange with protons is difficult. The effect of this exchange was studied by FTIR showing the intensity decrease of $\nu_{\text{C=O}}$ (–COOH), the carboxylic functional group band of the acid, and the shifting of ν_{as} (–COO[–]), the carboxylate functional group band under given pH and mercury conditions. For the FHA salt form, the characteristic band $\nu_{\text{C=O}}$ (–COOH) represented by a shoulder did not evolve, whereas the corresponding band to ν_{as} (–COO[–]) strongly shifted (40 cm^{–1}) for a maximum Hg²⁺ concentration (1 g l^{–1}). On the other hand, for the acid form (PFHA, LHA), the intense band of $\nu_{\text{C=O}}$ (–COOH) disappeared proportionally to the increase of Hg²⁺ concentration and the ν_{as} (–COO[–]) band moved for about 20 cm^{–1}. The same results were reached with pH variations. Our results were confirmed by ICP-AES mercury analysis. This study shows that humic acids react differently according to their chemical and structural state.

© 2008 Published by Elsevier B.V.

1. Introduction

Even though technology and industry are necessary for human welfare, they can seriously harm our environment. Soil pollution by heavy metals is a well known problem threatening nature as well as human health through under soil and surface water contamination [1]. Heavy metals are toxic at tiny amounts. Moreover, our industry contributes indirectly to their concentration on specific sites.

Billions of tonnes of mineral micropollutants are rejected every year. They contaminate the atmosphere (air), the hydrosphere (water) and the lithosphere (soil). They harm seriously the biosphere (living beings). The capacity of soil, a complex medium, to recycle effectively and quickly heavy metals, is under study [2]. For a long time studies were focused on the interaction of metals with clays [3–5]. However, in the last two decades, a special interest was

given to the organic part of soil and to its capacity to recycle heavy metals [6–9].

Clays and humic acids represent the major part of soil. Humic acids are natural organic compounds of soil. They result from the decomposition of organic matter. Their structure helps to fix heavy metals, to trap organic molecules and to oxidize or reduce compounds. Humic acid is composed of condensed nuclei related to each other by aliphatic chains (peptides, alkalis) and acid functional groups –COOH and phenolic –OH [10,11]. These two functional groups allow two types of interactions with heavy metals: carboxylate-metal cation and phenolate-metal cation [12–14]. If the interactions with metal are infrared exploited, it is not the same case with the phenol –OH function. The latter possesses a large band practically not exploitable [12,13]. Former work [15–18] and mainly work of Gossart et al. [17,19] showed that the interaction of the HA with Pb²⁺, Cd²⁺ and Zn²⁺ involves structural variations which can be followed by Fourier transform infrared (FTIR). We consequently carried out our work on the interactions of the humic acid with mercury in order to gather data for deeper soil investigations.

* Corresponding author.

E-mail address: a.addou@univ-mosta.dz (A. Addou).

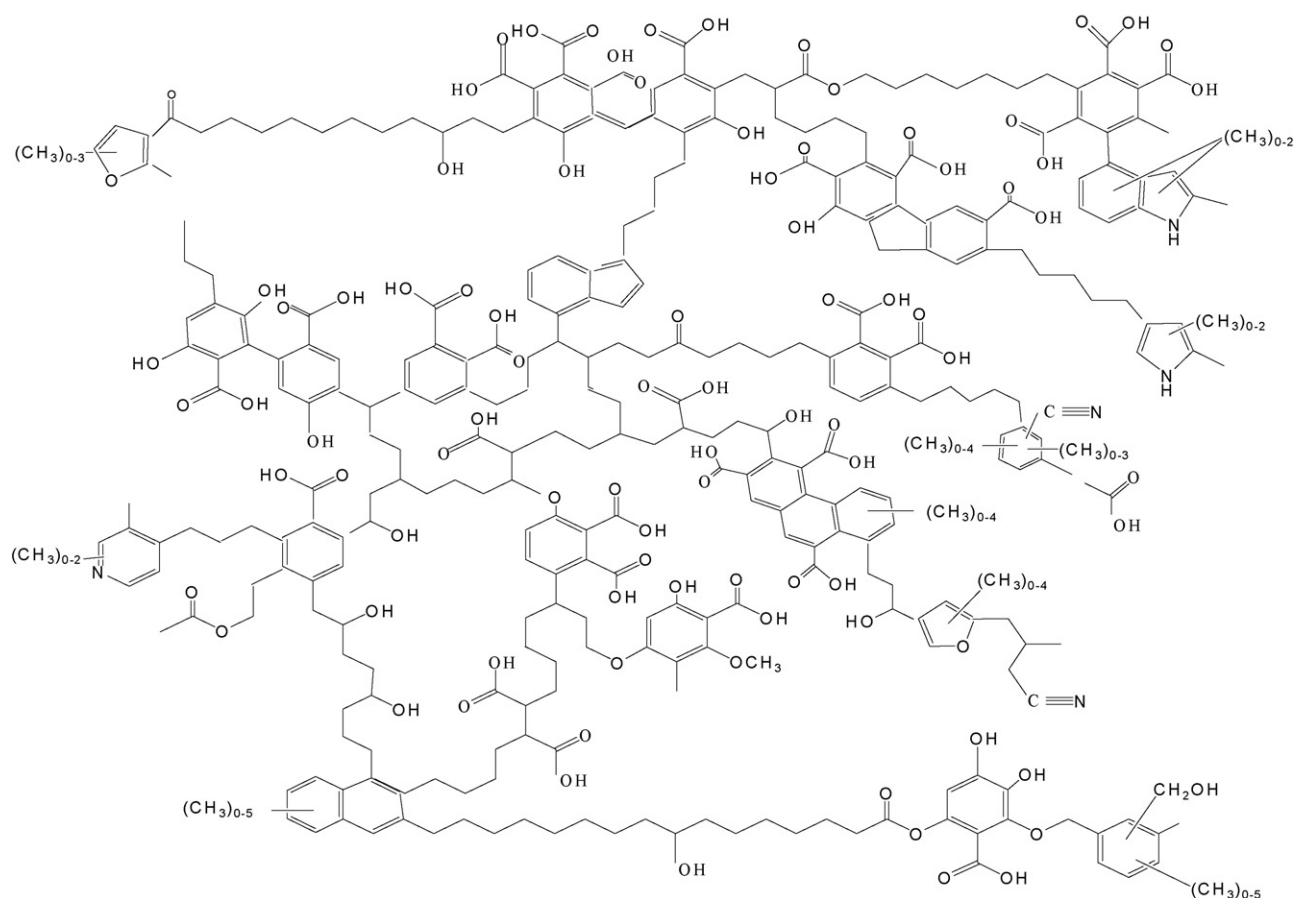


Fig. 1. Humic acid structure as proposed by Schulten and Schnitzer.

We carried out our study in a similar way than in previous works [17,19]: (i) study of the interactions model molecules–mercury for validation of the protocol and (ii) FTIR study of the interaction humic acid (HA)–mercuric ions (Hg^{2+}) under given conditions of pH and concentration [19]. HgO and Hg^{2+} are the most frequent states of mercury oxidation in the soil. The mercury contained in the soil is quickly immobilized in the form of carbonate or phosphate. It is fixed by oxide of iron, manganese and aluminium, [20–22] and especially by organic matter to which, it binds in the form of very stable organometallic complexes [23]. Structural data concerning humic acids is scarce. Nevertheless, models were proposed, giving an idea on the structure of this type of compound. A first model was imagined by Piccolo and Stevenson in 1982 [13]. Then, a second model was developed by Schulten and Schnitzer in 1993 [15]. This revealed that humic acids are complex macromolecules made up of aliphatic chains and several aromatic cycles which carry carboxylic and salicylic functional groups (Fig. 1). Gardea-Torresdey and co-workers [14,24,25] showed that the humic acid carboxylic groups are essentially responsible for the fixation phenomenon. Before studying the interaction HA–metals, we chose to study model molecules–metal interactions. These models are structurally close to humic acid and will allow a validation of the study. Benzoic acid and catechol, having the carboxylic acid functional group ($-\text{COOH}$) or the phenol functional group ($-\text{OH}$) grafted on aromatic cycles were selected like model molecules. Our study on HA–metal interactions was carried out with a humic acid marketed by FLUKA TM Company (FHA TM) and another coming from the International Humic Substances Society (IHSS TM). The study of the interactions humic acid–metal was carried out by Fourier transform

infra-red spectroscopy (FTIR). It allowed us to follow the variations of vibration frequencies of carboxylic functional groups observed in the average FTIR [14,26,27]. As in the study with lead, the vibration bands of carboxylic ($-\text{COOH}$) functional groups can undergo displacements and/or reductions in the intensities of absorption bands according to the nature and the concentration of the studied metal.

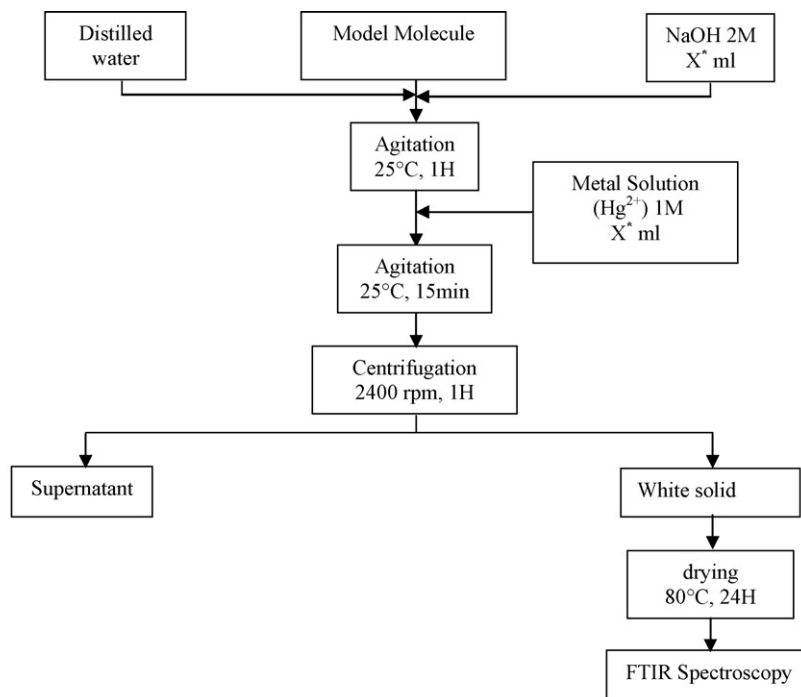
The main aim of this work is to understand: (i) the interactions of mercury with the carboxylic function, (ii) under which form (acid or salt) humic acid reacts efficiently with mercury and (iii) the affinity of humic acid towards mercury (mercury potential in sites occupation).

This study was supported by the analysis of metals by ICP-AES before and after each cation exchange.

2. Material and methods

2.1. Model molecules

Our study on the interaction model molecules–metal was carried out on the catechol $\text{C}_6\text{H}_4-(\text{OH})_2$, the benzoic acid $\text{C}_6\text{H}_5-\text{COOH}$ and the salicylic acid $\text{HO}-\text{C}_6\text{H}_4-\text{COOH}$ with Hg^{2+} . The benzoic acid, the catechol and the salicylic acid were provided by Merck Company TM. The mercury acetate comes from Fluka TM Company. First it was proceeded by a sodium exchange by adding a NaOH solution (2M). Then the sodium catecholate and benzoate obtained underwent an exchange $\text{Na}^+/\text{Hg}^{2+}$. The experimental protocol is detailed in Fig. 2. It is noteworthy that under the addition of the 1st drop of mercury acetate or lead nitrate, catecholate, benzoate



$X^* = 4$ ml for the model molecule benzoic acid .

$X^* = 9$ ml for the model molecule catechol.

$X^* = 7$ ml for the model molecule salicylic acid .

Fig. 2. Experimental protocol for the study of the interaction model molecule–metal.

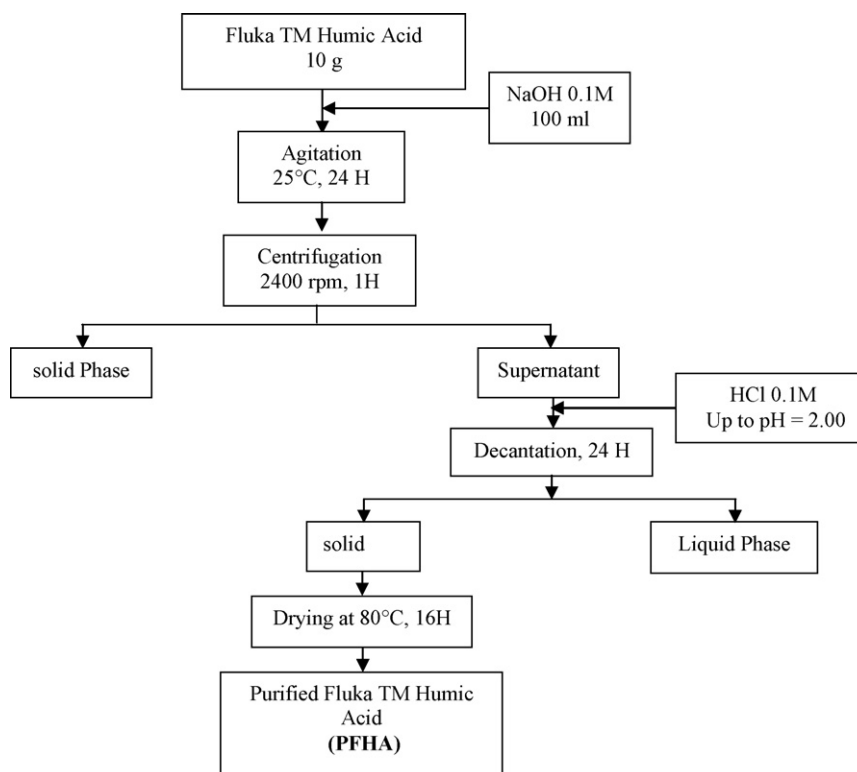
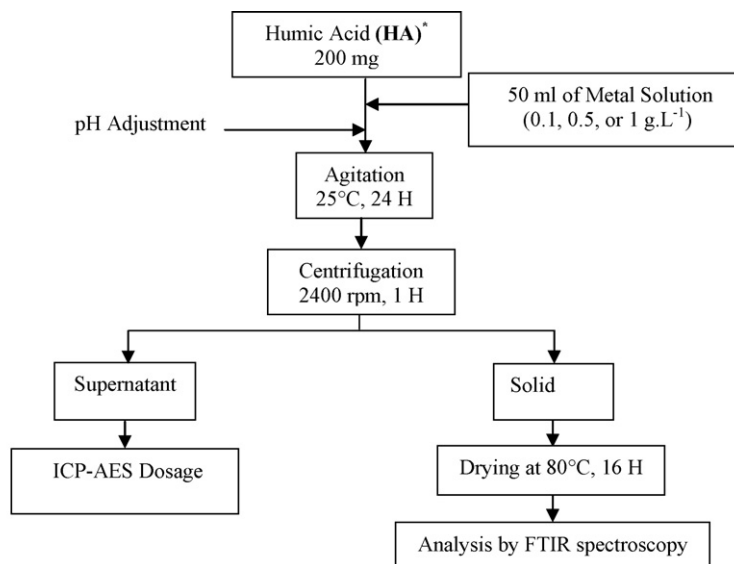


Fig. 3. Experimental protocol of Fluka TM humic acid (FHA) purification.



HA* = FHA, PFHA or LHA.

Fig. 4. Experimental protocol of the humic acid–metal interaction.

and salicylate Hg salts precipitated as a white solid, characteristic of certain mercury salts. The formation of these salts proved the exchange between Na^+ and Hg^{2+} ions. Salts were recovered after centrifugation and dried at 80°C (Fig. 2). A small fraction of each compound to be analyzed (1–2 mg) was pulverized then crushed in 100 mg of anhydrous KBr. The powder thus obtained was introduced into a mould to make pellets and was subjected to a pressure of $9.81 \cdot 10^8$ Pa in order to obtain a pellet of 13 mm in diameter. FTIR spectroscopic analysis was carried out in a spectrometer (Bruker YEWS 48) in the spectral domain $400\text{--}4000\text{ cm}^{-1}$ with a 4 cm^{-1} resolution.

2.2. Humic acids

In this work, humic acid, called FHA, came from Fluka TM company (batch no. 45729/1 50300) and Leonardite (LHA) was provided by the International Humic Substances Society (IHSS TM) whose protocol with NaOH and $\text{Na}_4\text{P}_2\text{O}_7$ extraction and subsequent HCl precipitation meets very strict standard requirements [28,29]. Leonardite is a brown coal from North Dakota. It is a low-cost material with potential as a heavy metal adsorbent. The humic acid (HA) from Leonardite has a molecular mass $M_w = 9637$ Da measured by gel permeation chromatography using an alkaline aqueous solution.

The elemental composition is: C% 53.78, H% 3.35, N% 2.09 and O% 40.0. The calculated molecular formula is $\text{C}_{420}\text{H}_{308}\text{N}_{14}\text{O}_{238}$ on the basis of the average molecular mass M_w [9,30–33].

2.3. FHA purification

The Fluka TM humic acid is marketed under the salt form. Its purification was carried out as indicated in Fig. 3. It was noted (PFHA). It was proceeded by dissolving 10 g of FHA in 100 ml of NaOH solution 0.1 M. The mixture was agitated during 24 h then centrifuged during 1 h at 2400 rpm. The soluble part obtained was acidified with a 0.1 M HCl solution until pH 2.00 which is the pH of humic acid precipitation [34]. After decantation, the precipitate was washed and dried at 80°C . This precipitate represents the purified Fluka TM humic acid called PFHA.

2.4. Interaction HA–metal

200 mg of each type of humic acid (FHA, PFHA or LHA) were added separately to 50 ml of mercury acetate solution at various concentrations 0.1, 0.5 and 1 g l^{-1} . It was studied at two different pH: (i): initial starting pH of the mixture where a partial dissolution is possible and (ii) pH was fixed at 3.00 by adjusting it with a solution of HCl (2 M) (Fig. 4). At this pH, humic acid does not dissolve. The mixture obtained was agitated during 24 h and then centrifuged with 2400 rpm. The insoluble part was dried at 80°C , then analyzed by FTIR spectroscopy. The recovered solutions after centrifugation were quantified by ICP-AES (Varian, axial view, liberty series V). The major mineral elements found in the soils such as: Na, Ca, Fe, Mg, Si and Al, in addition to mercury and lead were quantified [35].

Table 1
Frequencies assignment of model molecules and their salt form

Function	$\nu_{\text{C=O}} (-\text{COOH}) (\text{cm}^{-1})$	$\nu_{\text{C=O}} (-\text{COO}^-) (\text{cm}^{-1})$	$\nu_{\text{O-H}} (-\text{OH}) (\text{cm}^{-1})$	$\delta_{\text{O-H}} (-\text{OH}) (\text{cm}^{-1})$	$\nu_{\text{as}} (-\text{COO}^-) (\text{cm}^{-1})$	$\nu_{\text{s}} (-\text{COO}^-) (\text{cm}^{-1})$
Benzoic acid	1676	1230	2500–3200	–	–	–
Hg Benzoate	–	–	Disappearance	–	1496	1390
Catechol	–	–	3442 and 3318	1359	–	–
Hg Catechol	–	–	Disappearance	Disappearance	–	–
Salicylic acid	1658	1249	3200–3400	1380	–	–
Hg Salicylate	–	–	Disappearance	–	1554	1384

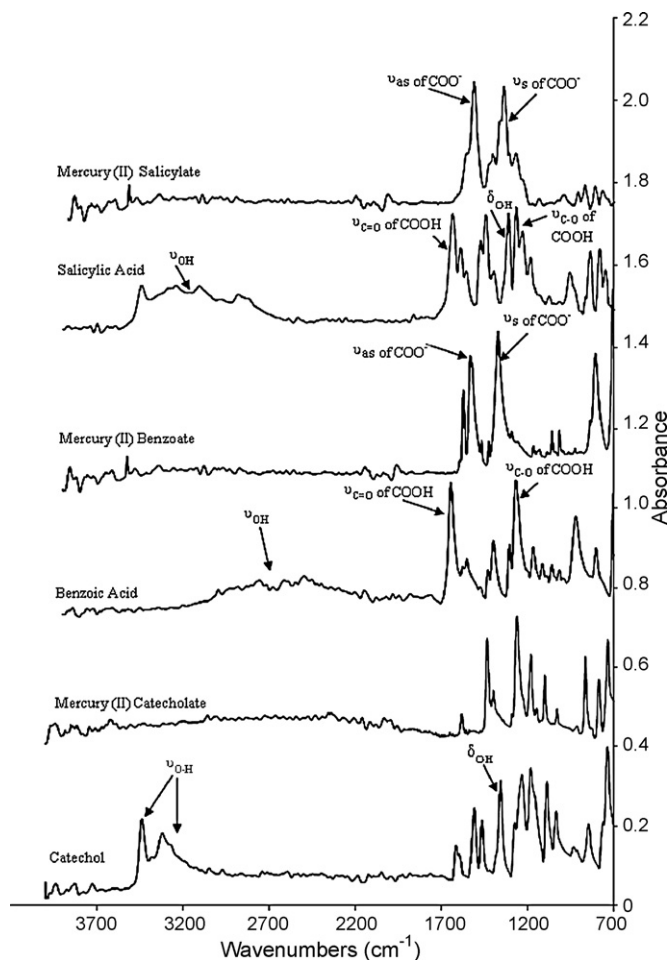


Fig. 5. FTIR spectra of model molecules and their shapes as mercury salts.

The ash contents of the humic samples are estimated by the following equation:

$$\text{ash}(\%) = \left(\frac{W_c}{W_d} \right) 100$$

where W_d is the weight of the dried humic sample and W_c the weight of the calcinated residue after heating at 800 °C for 6 h [36].

3. Results and discussion

3.1. Vibrational study of model molecules– Hg^{2+} interactions

FTIR spectra of benzoic acid, catechol and salicylic acid before and after fixation with mercury are represented in Fig. 5. Principal assignments are summarized in Table 1 in comparison with bibliographical data [37–42].

Stretch vibrations $\nu_{\text{C=O}}$ of the carboxylic acid functional group –COOH were observed in the wavenumbers 1716–1650 cm^{-1} domain and the stretch vibrations of $\nu_{\text{C=O}}$ of –COOH in the 1300–1250 cm^{-1} domain. For the phenol form, the two characteristic bands were the stretching and bending vibration of the hydroxyl functional group situated, respectively, in the 3400–3200 cm^{-1} and 1370–1350 cm^{-1} domains. The stretch frequency $\nu_{\text{C=O}}$ of benzoic acid was observed at 1676 cm^{-1} , the one corresponding to $\nu_{\text{C=O}}$ was observed at 1230 cm^{-1} . The elongation frequency $\nu_{\text{O-H}}$ appeared in the 3200–3400 cm^{-1} domain. For the catechol, the elongation vibrations ν_{OH} were located at 3442 cm^{-1} and 3318 cm^{-1} , the deformation vibration $\delta_{\text{O-H}}$ was observed at 1359 cm^{-1} (Table 1).

For salicylic acid, the $\delta_{\text{O-H}}$ deformation frequency appear at 1380 cm^{-1} (Fig. 5), and the elongation frequencies specific to $\nu_{\text{C=O}}$ and $\nu_{\text{C=O}}$ of –COOH appear at 1249 cm^{-1} and 1658 cm^{-1} , respectively. Also, the presence of $\nu_{\text{O-H}}$ vibrations between 3200–3400 cm^{-1} was noticed (Table 1).

If we compare FTIR spectra of the model molecules and salts obtained, we clearly notice the difference between the acid form (–COOH) and the carboxylate form (–COO[–]) and in the same way between the phenol and phenolate form. Indeed, the characteristic bands of the carboxylic acid functional group in the case of benzoic acid disappear by protons– Hg^{2+} exchange to give place to the characteristic bands of the carboxylate functional group which are assigned to the symmetrical and antisymmetrical stretch frequencies ν_s and ν_{as} (–COO[–]), respectively, vibrating in the 1550–1490 cm^{-1} and 1390–1330 cm^{-1} domains. In our study they are assigned to 1496 cm^{-1} for the antisymmetric stretch ν_{as} (–COO[–]) and to 1390 for the symmetrical elongation ν_s (–COO[–]) (Table 1).

For the catechol, the interaction with the mercuric ions leads to the catecholate whose two characteristic bands of stretch $\nu_{\text{O-H}}$ at 3442 and 3318 cm^{-1} and the one of deformation $\delta_{\text{O-H}}$ at 1359 cm^{-1} entirely disappear (Table 1). The same result was observed by Gosart et al. [17,19] with lead.

The Hg^{2+} salicylic acid interaction triggers the appearance of 1554 and 1384 cm^{-1} bands corresponding to ν_{as} and ν_s of –COO[–] of the mercury salicylate. Also the disappearance of the $\delta_{\text{O-H}}$ deformation and $\nu_{\text{O-H}}$ vibration bands specific to the –OH function of the formed salt was noticed. The displacement of the $\nu_{\text{C=O}}$ at 1384 cm^{-1} has hidden the one of $\delta_{\text{O-H}}$ already found at 1380 cm^{-1} .

The follow-up by FTIR spectroscopy of the characteristic bands of stretch ν_s and ν_{as} of the carboxylate functional group (–COO[–]) is better adapted than with OH functional group since the interaction mechanisms observed make it possible to better follow the variations at the level of frequencies associated with carboxylate functional groups (–COO[–]) by substitution of carboxylic functional groups (–COOH).

In the case of our study, the 1700–1400 cm^{-1} domain is characteristic of the –COOH function. However, in the 3400–3200 cm^{-1} region, the characteristic bands of OH and NH functions [38,43] were found because nitrogen is part of humic acid structure. A large band where it is difficult to relate interactions to spectroscopic studies was noticed in this region. Though OH region of salicylic acid

Table 2

Cation analysis and ash content in the studied humic acids

	Unit	Fluka humic acid (FHA)	Purified Fluka humic acid (PFHA)	Leonardite humic acid (LHA)
Na	mg kg ^{–1}	37,000	3800	2000
Ca	mg kg ^{–1}	22,000	3000	300
Fe	mg kg ^{–1}	14,000	4500	2000
Mg	mg kg ^{–1}	4400	0	40
Hg	mg kg ^{–1}	0	0	0
Si	mg kg ^{–1}	18,000	8300	150
Al	mg kg ^{–1}	9000	4200	2500
Ash content	% Mass	19.70	3.50	2.58

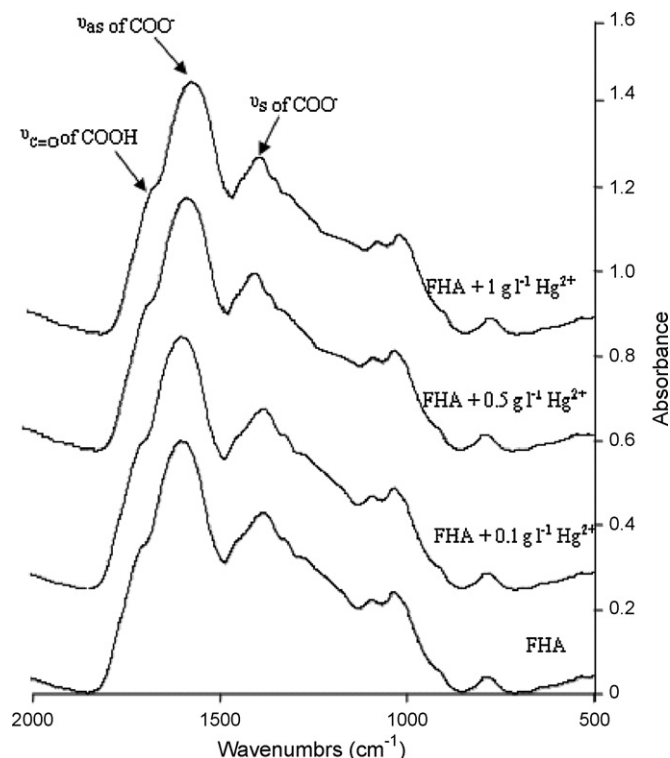


Fig. 6. FTIR spectra of FHA and its mercury salt form.

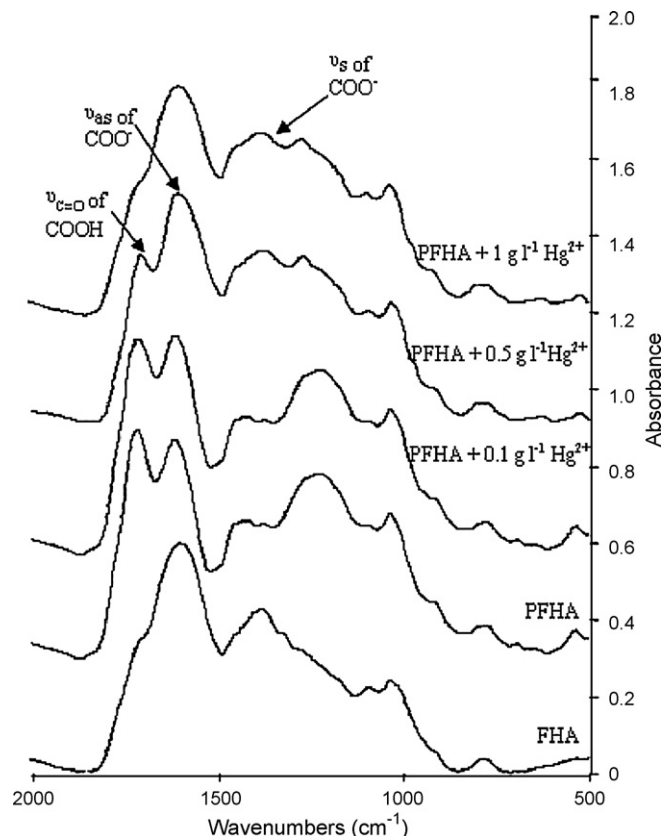


Fig. 7. FTIR spectra of FHA, PFHA and its mercury salt form (0.1, 0.5 and 1 g l⁻¹).

was markedly changed upon interaction with Hg, this band was not used in study of humic–Hg interaction because of its strong overlap with humic amine vibrations.

Dupuy and Douay [18] showed that the 1700–1400 cm⁻¹ spectral window is very important for the correlation between the absorbencies and the pollution level.

The choice of the FTIR study, supported by the work of Gossart et al. [17–19] for the evaluation of events observed at the time of the molecules–Hg²⁺ interaction appears to us completely adapted for the study and interpretation of soil contamination by heavy metals fixed on humic acid.

3.2. Study of the Fluka™ humic acids (FHA) and Leonardite Humic Acid (LHA): ICP-AES analysis and FTIR analysis

3.2.1. Fluka™ humic acid (FHA)

FHA contains a great number of impurities. The high rates of Si, Fe and Al showed a strong mineral proportion generally under the form of silica, alumina and iron oxide. The ash content is about 20% (Table 2). The FHA also contains a large quantity of Na (37,000 mg kg⁻¹) and Ca (22,000 mg kg⁻¹) (Table 2). Their presence is certainly due to the extraction mode using alkaline treatment. The analysis results showed that the FHA is rather a calcium and sodium salt. For these reasons, we were obliged to purify the FHA.

Table 3
Spectra principal bands assignment of FHA, PFHA, LHA and LHA standard (IHSS)

Attribution	Unit	FHA	PFHA	LHA	LHA standard (IHSS)
$\nu_{C=O}$ Carboxylic	cm ⁻¹	1695	1715	1709	1713
$\nu_{C=O}$ Asymmetric carboxylate	cm ⁻¹	1590	1610	1608	1609
$\nu_{C=O}$ Symetric carboxylate	cm ⁻¹	1386	1420	1429	1382
$\nu_{C=O}$ Carboxylic	cm ⁻¹	–	1224	1232	1214
ν_{Si-O} Silica	cm ⁻¹	1031	1031	–	–

The study of the spectra shows a rather salt form (carboxylate –COO⁻) than acid form (–COOH) and a mineral part.

- (I) Acid form: a shoulder at 1695 cm⁻¹ corresponding to the stretch $\nu_{C=O}$ (–COOH) (Fig. 6 and Table 3) was noticed instead of an intense peak as for the benzoic acid ($\nu_{C=O}$ at 1676 cm⁻¹) (Fig. 5).
- (II) Salt form: the stretch frequency ν_{as} (–COO⁻) was observed at 1590 cm⁻¹ for the FHA (Fig. 6) whereas it was at 1496 cm⁻¹ for Hg benzoate and the ν_s (–COO⁻) appeared at 1386 cm⁻¹ (1390 cm⁻¹ for Hg benzoate). The absence of the $\nu_{C=O}$ (–COOH) band in the domain 1250–1350 cm⁻¹ was noticed, thus confirming the salt form of the FHA instead of a “pure” acid form.
- (III) Mineral part: the characteristic absorption band ν_{Si-O} of silica was observed at 1031 cm⁻¹ [38,41,43,44] confirming the presence of the mineral part of FHA (Fig. 6 and Table 3).

3.2.2. Purified Fluka™ humic acid (PFHA)

The FHA purification caused a strong loss of cations as shown by the ICP-AES results (Table 2). The sodium and the calcium quantities decreased by 90% and 98%, respectively, and the ash amount decreased by more than 80%. The purification (acidification) is confirmed on the infra-red spectra (Fig. 7) since the

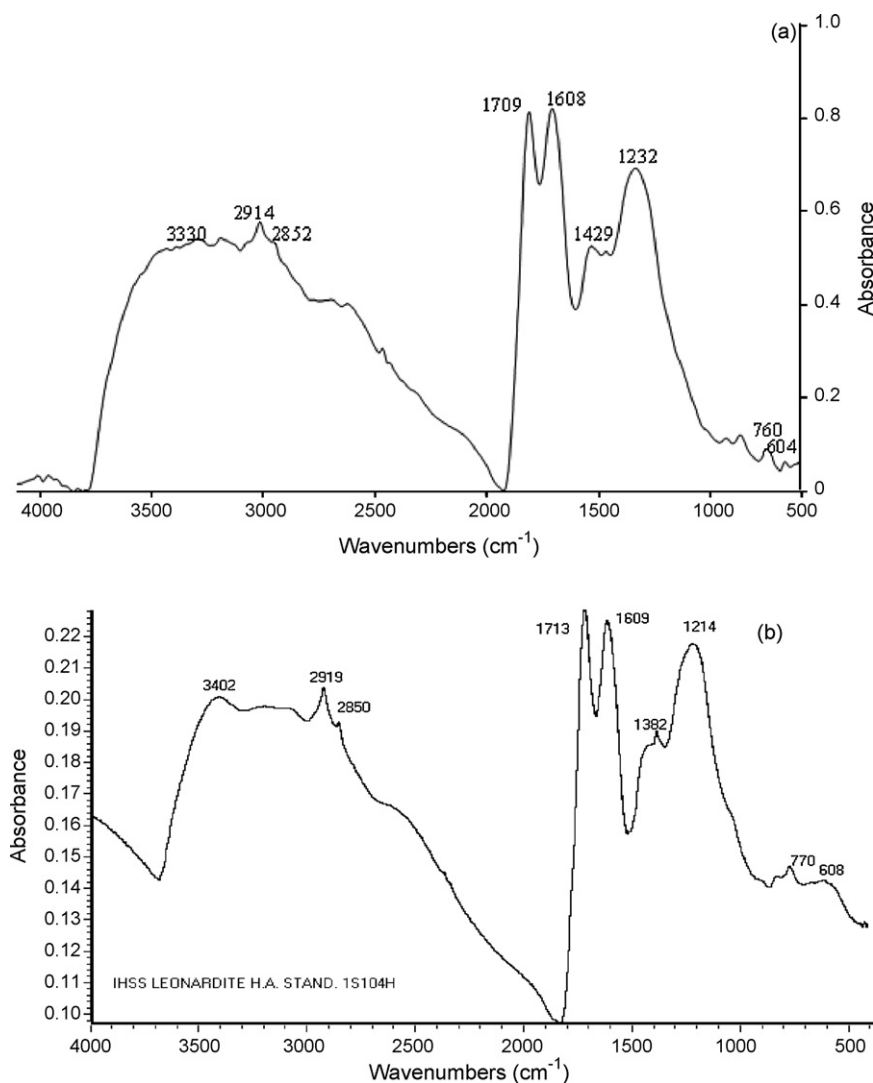


Fig. 8. (a) FTIR spectra of LHA, and (b) FTIR spectra of LHA standard (IHSS).

shoulder at 1695 cm^{-1} disappeared giving place to the intense peak at 1715 cm^{-1} corresponding to $\nu_{\text{C=O}}$ ($-\text{COOH}$) characteristic of the acid form and the reappearance of the peak corresponding to the $\nu_{\text{C=O}}$ ($-\text{COOH}$) at 1224 cm^{-1} confirms the acid form of the PFHA (1676 and 1230 cm^{-1} for the benzoic acid). The frequency ν_{as} ($-\text{COO}^-$) was subject to a displacement from 1590 cm^{-1} to 1610 cm^{-1} (Table 3).

3.2.3. Leonardite humic acid (LHA)

LHA contains fewer impurities than the two previous humic acids. The ash content is about 3% (Table 2). This good level of purity is due to the good quality of humic acids contained in the initial extract. The results obtained by ICP-AES quantification of the LHA show that the principal minerals found in the soil are much weaker in this acid. As example the silica rate in LHA (150 mg kg^{-1}) is 100 times weaker than in FHA (18000 mg kg^{-1}) and 50 times weaker than in PFHA (8300 mg kg^{-1}).

Fourier transform infrared spectra are presented in Fig. 8a. It has a profile close to that of the PFHA, the assignment of the principal bands of the three acids is given on Table 3 with:

- (i) an acid form: $\nu_{\text{C=O}}$ ($-\text{COOH}$) at 1709 cm^{-1} and $\nu_{\text{C=O}}$ ($-\text{COOH}$) at 1232 cm^{-1} ,

- (ii) a salt form: ν_{as} ($-\text{COO}^-$) at 1608 cm^{-1} , ν_{s} ($-\text{COO}^-$) at 1429 cm^{-1} , values close to those found for the PFHA and
- (iii) absence of the peak corresponding to silica.

This acid has an FTIR spectrum (Fig. 8a) showing a high level of organic matter. It looks like the IRTF spectrum of the humic acid Leonardite standard IHSS (Fig. 8b and Table 3). This report is important since it will make it possible to correctly study the behaviour of the organic matter (LHA) at the time of an interaction with mercury and to observe the spectral modifications without important interference of the mineral matter. It should be noticed that the mineral part of the soil has also a strong capacity of metals fixation [45]. A previous work showed that the proton exchange $\text{H}^+ - \text{Pb}^{2+}$ could be followed by the displacement of the frequency ν_{as} and ν_{s} of ($-\text{COO}^-$) and the intensity of the peak characteristic of the frequency $\nu_{\text{C=O}}$ ($-\text{COOH}$) at 1715 cm^{-1} (Figs. 7 and 9) [17].

3.3. Humic acid–mercuric ion interaction

The study of the interaction of various humic acids (FHA, PFHA, LHA) with mercuric ion was carried out according to the concentrations of Hg and the pH. The results are represented in Table 4.

Table 4
Chemical characterization of the mercury sorption by the studied humic acids

	Hg Concentration			
	0 g l ⁻¹	0.1 g l ⁻¹	0.5 g l ⁻¹	1 g l ⁻¹
FHA				
Initial pH	5.45	5.27	5.03	4.80
Final pH	6.50	6.20	5.22	4.25
Hg Mass sorption (mg)	0.0	4.55	23.75	49.50
% of sorption		91	95	99
$\nu_{as}(-COO^-) cm^{-1}$	1590	1580	1565	1550
$\nu_s(-COO^-) cm^{-1}$	1386	1390	1401	1405
Characteristics of COOH	No variation	No variation	No variation	No variation
Initial pH	3.00	3.00	3.00	3.00
Final pH	6.21	5.68	4.73	3.78
Hg Mass sorption (mg)	0.0	4.55	23	47
% of sorption		91	92	94
$\nu_{as}(-COO^-) cm^{-1}$	1587	1576	1567	1553
$\nu_s(-COO^-) cm^{-1}$	1385	1385	1395	1400
Characteristics of COOH	No variation	No variation	No variation	No variation
PFHA				
Initial pH	5.48	5.11	4.85	4.59
Final pH	2.97	2.76	2.38	2.10
Hg Mass sorption (mg)	0.0	4.95	21.75	41.00
% of sorption		99	87	82
$\nu_{as}(-COO^-) cm^{-1}$	1612	1611	1605	1590
$\nu_s(-COO^-) cm^{-1}$	1420	1423	1427	1430
Characteristics of COOH	Appearance	Decrease	Important decrease	Almost total disappearance
Initial pH	3.00	3.00	3.00	3.00
Final pH	2.72	2.44	2.27	2.00
Hg Mass sorption (mg)	0.0	4.90	21.25	40.00
% of sorption		98	85	80
$\nu_{as}(-COO^-) cm^{-1}$	1613	1609	1604	1597
$\nu_s(-COO^-) cm^{-1}$	1417	1423	1425	1426
Characteristics of COOH	Appearance	Decrease	Important decrease	Almost total disappearance
LHA				
Initial pH	5.60	5.00	4.98	4.96
Final pH	3.16	2.92	2.50	2.20
Hg Mass sorption (mg)	0.0	4.85	19.00	35.00
% of sorption		97	75	70
$\nu_{as}(-COO^-) cm^{-1}$	1610	1608	1599	1591
$\nu_s(-COO^-) cm^{-1}$	1429	1432	1436	1441
Characteristics of COOH	Appearance	decrease	Important decrease	Almost total disappearance
Initial pH	3.00	3.00	3.00	3.00
Final pH	2.89	2.70	2.35	2.27
Hg Mass sorption (mg)	0.0	4.90	19.75	37.00
% of sorption		98	79	74
$\nu_{as}(-COO^-) cm^{-1}$	1612	1611	1588	1581
$\nu_s(-COO^-) cm^{-1}$	1425	1428	1435	1435
Characteristics of COOH	Appearance	Decrease	Important decrease	Almost total disappearance

3.3.1. Fluka TM humic acid–mercuric ion interaction

3.3.1.1. Effect of mercury concentration and pH. The fixation percentage of mercury increases according to the concentration of Hg²⁺ which increases from 91 to 99% (Table 4) at initial pH and from 91 to 94% at pH 3. For 0.1 and 0.5 g l⁻¹ concentrations, the increase in the pH results in the exchange between Hg²⁺ and Na⁺, Ca²⁺, which is confirmed by quantifying Na⁺ and Ca²⁺ cations (Table 5).

For the maximum concentration of Hg²⁺ (1 g l⁻¹) the reduction in the pH (Table 4) is due to the Hg²⁺/H⁺ exchange since the ini-

tially occupied sites by Na⁺, Ca²⁺ were saturated by Hg²⁺ at 0.1 and 0.5 g l⁻¹ concentrations.

3.3.1.2. Vibrational study by FTIR. The concentration effect of Hg²⁺ caused a shift towards the low wavenumbers of the band corresponding to the stretch $\nu_{as}(-COO^-)$ of the carboxylate form (salt) of FHA. Indeed, the latter shifted from 1590 to 1550 cm⁻¹, that is to say a move of 40 cm⁻¹ for the maximum concentration (1 g l⁻¹) and an initial pH of 5.45. When the pH was decreased to 3, the exchange became more difficult between the protons and the mercuric ions, as confirmed by analytical quantification (Table 4) and a weaker shift following the increase of Hg²⁺ concentration (shift of 34 cm⁻¹ for 1 g l⁻¹) was noticed. In the interaction with Pb²⁺, the shift was even weaker, about 26 cm⁻¹ for an initial pH of 5.42 and 23 cm⁻¹ for an imposed pH of 3 [17]. However, the intensity corresponding to $\nu_{C=O}(-COOH)$ did not change (Fig. 6), whatever the concentration and the pH were, which proves the salt form of FHA. We can deduce that FHA cation exchange with mercury involves a more important shift at the level of the characteristic peak of the carboxylate form $\nu_{as}(-COO^-)$ than with lead. Also we notice a $\nu_{C=O}$ shift from 1386

Table 5
Cation analysis in the: FHA–1 g l⁻¹ Hg, PFHA–1 g l⁻¹ Hg and LHA–1 g l⁻¹ Hg

Unit	FHA + Hg ²⁺ (1 g l ⁻¹)	PFHA + Hg ²⁺ (1 g l ⁻¹)	LHA + Hg ²⁺ (1 g l ⁻¹)
Na mg kg ⁻¹	2000	1000	170
Ca mg kg ⁻¹	7600	100	0
Fe mg kg ⁻¹	11,000	2900	995
Mg mg kg ⁻¹	1500	0	0
Hg mg kg ⁻¹	2,48,750	2,08,000	1,75,000
Si mg kg ⁻¹	15,000	<8300	<150
Al mg kg ⁻¹	6500	<4200	<2500

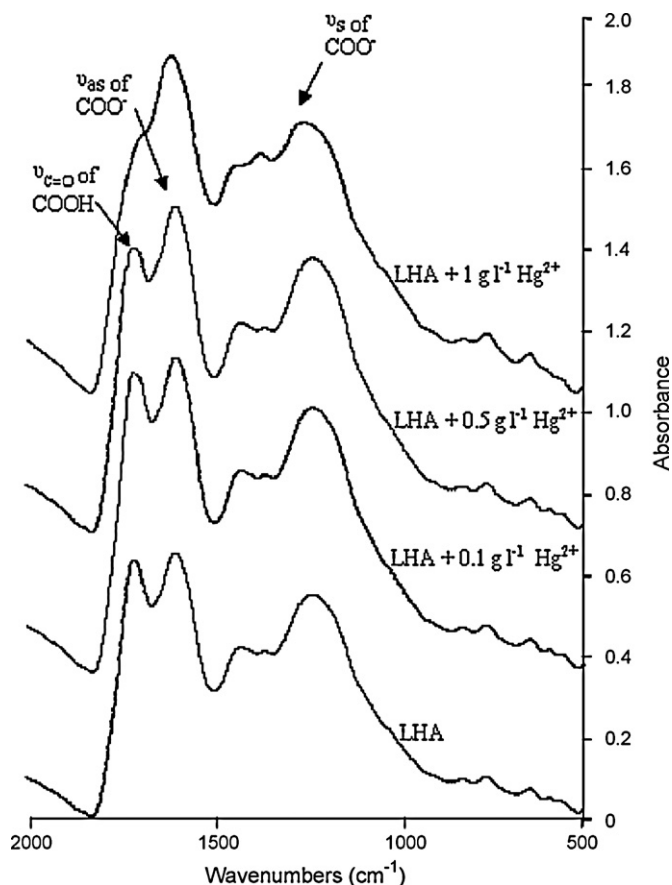


Fig. 9. FTIR spectra of LHA and its mercury salt form (0.1, 0.5 and 1 g l⁻¹).

to 1410 cm⁻¹. Thus we would be able to have an initial fast qualitative answer concerning the nature of the metal exchanged (Hg²⁺ or Pb²⁺) according to the importance of the frequency shift of the band $\nu_{\text{as}}(-\text{COO}^-)$.

For the $\nu_{\text{s}}(-\text{COO}^-)$ bands, we notice a shift towards high values wavenumbers reaching up to 20 cm⁻¹. Indeed, for a sorption of Hg (1 g l⁻¹), the $\nu_{\text{s}}(-\text{COO}^-)$ shift from 1386 to 1405 cm⁻¹. It is relatively weak compared to $\nu_{\text{as}}(-\text{COO}^-)$.

3.3.2. Purified Fluka TM humic acid (PFHA)–mercuric ion interaction

3.3.2.1. Effect of the concentration and the pH. At weak Hg²⁺ concentrations (0.1 g l⁻¹), the exchange is almost total (99%). This is explained by the availability of Na⁺ and Ca²⁺ ions which decreased after purification (Table 2) and which was exchanged by Hg²⁺. On the other hand, when the Hg²⁺ concentration increases, PFHA is under acid form, the exchange is more difficult because of the competition Hg²⁺/H⁺. The pH of the solution decreases very slightly (2.30 and 2.10) confirming a limited exchange. With pH equal to 3, the ratio of exchange is much weaker and reaches only 80% with a final pH of 2.00. This confirms the competitiveness Hg²⁺/H⁺ on the sites occupied by the protons of PFHA.

3.3.2.2. Vibrational study. In this case also an evolution in the shift of the frequency band $\nu_{\text{as}}(-\text{COO}^-)$ towards the low wavenumbers per effect of the concentration in Hg²⁺ was observed. A maximum shift of 20 cm⁻¹ was noticed since $\nu_{\text{as}}(-\text{COO}^-)$ goes from 1612 to 1590 cm⁻¹ for the maximum Hg concentration (1 g l⁻¹). Contrary to FHA, the effect of the mercury concentration showed that the intensity of the $\nu_{\text{C=O}}(-\text{COOH})$ band at 1715 cm⁻¹, characteristic of

the acid functional group ($-\text{COOH}$) of the PFHA, decreases with the increase in the mercury concentration until its total disappearance (for [Hg²⁺] = 1 g l⁻¹). Also we notice a decrease and a shift of $\nu_{\text{s}} \text{COO}^-$ band. This result was mentioned by Klucakova [14]. There is an intensity diminution and a $\nu_{\text{C=O}}$ shift from 1224 to 1420 cm⁻¹. The latter is close to 1410 cm⁻¹ in the case of AHF 1 g l⁻¹ Hg. It shows that all the sites are occupied by mercury in COOH.

This intensity reduction is explained by the exchange between the protons and the mercuric ions until obtaining the salt form of PFHA (Fig. 7).

Thus the aspect of the FHA spectra was found. This result differs from the one found with PFHA–Pb²⁺ interactions [17] where this characteristic band does not disappear whatever the pH and the lead concentration were.

3.3.3. Leonardite humic acid (LHA)–mercuric ion interaction

3.3.3.1. Effect of the concentration and the pH. The sorption rates for the mercury concentrations 0.1 and 0.5 g l⁻¹ are 97% and 75%, respectively. With the maximum concentration 1 g l⁻¹, the percentage of mercury fixation decreases to 70%, which shows that the cation exchange is limited by the competition Hg²⁺/H⁺. Indeed, LHA being under acid form, the calcium and sodium rates which are weaker compared to the two other humic acids involve weak variations of exchange with Hg²⁺. With a more acid pH (3), a more difficult exchange was noticed, which is explained by a weaker release of protons compared to the PFHA (Table 4).

3.3.3.2. Vibrational study. LHA being under acid form has an almost identical vibrational behaviour to that of PFHA. Indeed, the shift of the $\nu_{\text{as}}(-\text{COO}^-)$ band was observed according to the concentration effect. From 1610 it shifts to 1591 cm⁻¹, that is 19 cm⁻¹ (same shift as for PFHA) for the initial pH and up to 31 cm⁻¹ for the pH equal to 3. For the frequency $\nu_{\text{C=O}}(-\text{COOH})$ at 1709 cm⁻¹, its intensity decreases until its total disappearance for the maximum Hg²⁺ concentration. This once more confirms the acid form of LHA which evolves to the salt functional group according to the exchange with mercuric ions. With lead, we notice a shift of 12 and 7 cm⁻¹, respectively for the initial pH and pH 3.

3.4. Summary discussion

The study of the interaction simple model molecule–mercuric ion by FTIR spectroscopy showed the disappearance of the band corresponding to the carboxylic functional group leaving place to the mercury carboxylate salt functional group. This is regarded as the principal index of the metal fixation in the study of humic acid–mercuric ions interaction. For a given humic acid, there are relationships between the fixed mercury mass and certain infrared spectra bands. Two behaviours were observed for the studied humic acids:

- (I) The FHA fixed the maximum of Hg²⁺ (99%) at the maximum mercury concentration (1 g l⁻¹) because of easy exchange between Na⁺ and Ca²⁺ which occupies the FHA sites in salt form. These exchanges were followed by the shift of the frequency $\nu_{\text{as}}(-\text{COO}^-)$ towards low wavenumbers according to mercury concentration where a shift of 40 cm⁻¹ was noted. The study with lead gave a shift of 20 cm⁻¹. Also there is an intensity decrease and a shift of $\nu_{\text{C=O}}$ from 1232 to 1415 cm⁻¹.
- (II) Acid forms PFHA, LHA, by the nature of their structure and their “pure” acid form, showed limited rates of mercury fixation because of the occupied sites with more protons. The difficulty of exchange of the latter with metal ions was confirmed. However, this exchange followed by FTIR gave a shift of the carboxylate band $\nu_{\text{as}}(-\text{COO}^-)$ and a reduction in the

intensity of $\nu_{C=O}$ ($-COOH$) by effect of the mercury concentration until its total disappearance. This result differs from the one obtained with lead since the frequency $\nu_{C=O}$ ($-COOH$) does not disappear even with maximum concentration of lead. This behavioural difference of Pb^{2+} and Hg^{2+} towards humic acid is explained by the weak ionic ray of mercury (Hg^{2+} $r=0.83 \text{ \AA}$) and its greater affinity compared to that of lead (Pb^{2+} $r=1.33 \text{ \AA}$) [7,46].

4. Conclusion

This vibrational study by FTIR, which supplements that of Gosart et al., is a tool for fast prospecting of pollution by mercury and lead in the organic part of the soil. To our knowledge, an extraction of the humic acid, followed by the realization of an infra-red spectrum, would direct us towards the detection of a contamination by lead or mercury. We would study only the values of the frequencies of the carboxylate bands ν_{as} ($-COO^-$) and the intensities of $\nu_{C=O}$ ($-COOH$) corresponding to the humic acids/mercury or lead complexes. In the future, it would be interesting to see the competition of these two heavy metals for fixation with humic acid for an extrapolation of a possible individual or mixed contamination by mercury and/or lead. We can conclude that, at this level of investigation, the analytical and spectroscopic protocols used in this work, in complement with those used with lead, could be developed.

References

- [1] I.S. Kim, Y.S. Choi, A. Jang, Remediation of polluted soil and sediment: perspectives and failures, in: Proceedings of First International Conference on Environmental Restoration, Ljubljana, Slovenia, 1997, pp. 83–90.
- [2] R. Gras, Soil Physics for Preparation, Masson, Paris, Milan, 1988.
- [3] H. Hohl, W. Stumm, J. Colloid Interface Sci. 55 (1976) 281.
- [4] J.A. Davis, J.O. Leckie, J. Colloid Interface Sci. 63 (1978) 480.
- [5] M.M. Benjamin, J.O. Leckie, J. Colloid Interface Sci. 83 (1981) 410.
- [6] M.A.T. Van den Hoop, H.P. Van Leeuwen, J.P. Pinheiro, A.M. Mota, M.de.L. Simoes Gonçalves, Colloids Surfaces A: Physicochem. Eng. Aspects. 95 (1995) 305–313.
- [7] A. Liu, R.D. Gonzalez, J. Colloid Interface Sci. 218 (1999) 225–232.
- [8] M.L.H. Aim, P. Conte, A. Piccolo, Chemosphere 52 (2003) 265–275.
- [9] Z. Zeledon-Toruno, C. Lao-Luque, M. Solé-Sardans, J. Chem. Technol. Biotechnol. 80 (2005) 649–656.
- [10] L. Beyer, Zeitschrift Pflanz. Bodenkunde. 159 (6) (1996) 527–539.
- [11] K. Haider, J. Plant Nutr. Soil Sci. 162 (4) (1999) 363–371.
- [12] M. Schnitzer, S.I.M. Skinner, Soil Sci. 99 (1965) 278.
- [13] A. Piccolo, F.J. Stevenson, Geoderma 27 (1982) 195.
- [14] M. Klucakova, P. Pelikan, L. Lapcik, B. Lapcikova, J. Kucerik, M. Kalab, J. Mater. Polym. Mater. 17 (2000) 337.
- [15] H.R. Schulten, M. Schnitzer (Ed.), A state of the art structural concept for humic substances, Nature, Wissens Chaften, 80, 1993, pp. 29–30.
- [16] M.G. Perez, Geoderma 118 (2004) 181–190.
- [17] P. Gossart, A. Semmoud, B. Ouddane, J.-P. Huvenne, Phys. Chem. News 9 (2003) 101–108.
- [18] N. Dupuy, F. Douay, Spectrochim. Acta Part A 57 (2001) 1037–1047.
- [19] P. Gossart, A. Semmoud, C. Ruckebusch, J.-P. Huvenne, Anal. Chim. Acta 224166 (2002) 1–9.
- [20] G. Fu, H.E. Allen, Water Res. 26 (1992) 225.
- [21] J.L. Zhou, S. Rowland, R.F.C. Mantoura, J. Braven, Water Res. 28 (1994) 571.
- [22] A.P. Davis, M. Upadhyaya, Water Res. 30 (1996) 1894.
- [23] Y. Chen, Organic matter reactions involving micronutrients in soils and their effect on Plants, in: A. Piccolo (Ed.), Humic Substances in Terrestrial Ecosystems, Elsevier, Amsterdam, 1996, pp. 507–530.
- [24] J.L. Gardea-Torresdey, K.J. Tiemann, J.H. Gonzalez, J.A. Hennig, M.S. Townsend, J. Hazard. Mater. 48 (1996) 181.
- [25] J.L. Gardea-Torresdey, L. Tang, J.M. Salvador, J. Hazard. Mater. 48 (1996) 191.
- [26] M. Schnitzer, Soil. Sci. 151 (1991) 41.
- [27] L.L. Shevchemko, Russ. Chem. Rev. 32 (1963) 201.
- [28] M.H.B. Hayes, in: G.R. Aikem, D.M. McKnight, R.L. Wershaw, P. McCarthy (Eds.), Humic Substances in Soil, Sediment and Water, Wiley, New York, 1985, pp. 329–362.
- [29] R.S. Swift, Organic matter characterization. Methods of Soil Analysis. Part 3. Chemical Methods—SSSA Book Series, vol. 5. SSSA, Madison, WI, 1996, pp. 1011–1069.
- [30] G.J. Lawson, D. Stewart, Coal humic acid, in: M.H.B. Hayes, Q. MacCarty, R.L. Malcom, R.S. Swift (Eds.), Humic Substances II, Search of structures, 4, Wiley, New York, 1989, p. 641.
- [31] G. Ricca, L. Federico, C. Astori, R. Gallo, Geoderma 57 (1993) 263–274.
- [32] F. Severini, G. Ricca, K. Franchi, in: Bari, N. Senesi, T. Miano (Eds.), Proceedings of the Third National Congress IHSS T.M., Facoltà di agrarian, Università di bari Publishers, 1995.
- [33] C. Pastorelli, L. Formaro, G. Ricca, F. Severini, Colloids Surfaces B: Biointerface 13 (1999) 127–134.
- [34] C. Liao, M. Lu, S. Su, Chemosphere 44 (2001) 913–919.
- [35] M. Pansu, J. Gautheyrou, J.-Y. Loyer, Soil Analysis: Sampling, Instrumentation and Control, Masson, Paris, 1998, pp. 205–229.
- [36] X.Q. Lu, J.V. Hanna, W.D. Johnson, Appl. Geochem. 15 (2000) 269.
- [37] G. Barancikova, N. Senesi, G. Brunetti, Geoderma 78 (1997) 251–266.
- [38] F.J. Stevenson, Humus Chemistry: Genesis, Composition, Reaction, Wiley, New York, 1994.
- [39] R.M. Silverstein, G.C. Bassler, T.C. Morrill, Spectrometric Identification of Organic Compounds, Wiley, New York, 1991.
- [40] M. Schnitzer, S.U. Khan, Soil Organic Matter, Elsevier, Amsterdam, 1978.
- [41] M. Schnitzer, S.U. Khan, Humic Substances in the Environment, Marcel Dekker, New York, 1972.
- [42] M. González Pérez, L. Martin-Neto, S.C. Saab, E.H. Novotny, D.M.B.P. Milori, V.S. Bagnato, L.A. Colnago, W.J. Melo, H. Knicker, Geoderma 118 (2004) 181–190.
- [43] P. MacCarthy, J.A. Rice, et al., Spectroscopic methods (other than NMR) for determining functionality in humic substances, in: G.R. Aiken (Ed.), Humic Substances in Soil Sediment, and Water, Wiley-Interscience, New York, 1985, pp. 527–559.
- [44] D.C. Olk, G. Brunetti, N. Senesi, Soil Sci. 164 (1999) 649–663.
- [45] M. Robert, The Soil: Interface in Environment, Resource for Development, Masson, Paris, 1996.
- [46] T.A.O' Shea, K.H. Mancy, Water Res. 12 (1978) 703.